Peracetic Acid Treatment as an Effective Method to Protect Wood Discoloration by UV Light

Kyoung-Chan PARK[1] · Byeongho KIM[1] · Hanna PARK[1] · Se-Yeong PARK[1,†]

ABSTRACT

Wood has always been used for various day-to-day applications such as interior or exterior construction materials, and household products. However, it can undergo photodegradation and discoloration by environmental factors including ultraviolet (UV) light, and thus has shortened its service life. Bleaching or delignification of wood surfaces is a suitable solution to stabilize wood against weathering by UV because these techniques can alter or remove the chromophores in lignin, which is a main factor of wood discoloration. To improve the color stability of wood surface according to the lifespan, surface delignification was conducted using peracetic acid (PAA) and hydrogen peroxide (HP) on the woods of *Larix kaempferi* and *Quercus mongolica*. After the PAA treatment, L^* increased considerably from 60−70 to 90−95. Furthermore, wood surface color did not change significantly after UV exposure. The color differences (ΔE^*) between before and after PPA treatment of wood showed the 4.8−12.2 of *L. kaempferi*, and 1.7−3.7 of *Q. mongolica*, respectively. The lignin-related peaks in Fourier transform infrared spectroscopy (FT-IR) spectra disappeared with increased duration of PAA treatment. These results confirmed that the lignin component was partially or completely removed after the PAA treatment; the color differences (ΔE^*) clearly showed that there was a reduction in redness (a^*) and yellowness (b^*), and an increase in lightness (L^*) owing to the removal of lignin. Based on these results, this study demonstrated that the partial removal of lignin from wood surfaces is a fundamental method for resolving photo-degradation.

Keywords: peracetic acid, photostabilization, delignification, bleaching, ultraviolet (UV) exposure, discoloration, wood surface treatment

1. INTRODUCTION

Wood, a renewable resource and a natural polymer, is gaining increasing global attention as part of the collective effort to mitigate climate change. As one of the most abundant resources on the planet, wood has long been used for various applications such as interior and exterior construction material, household products, and fuel. Until recently, research has been conducted on fuel and exterior building materials such as CLT, plywood, MDF, etc (Fujimoto *et al.*, 2021; Jang and Lee, 2019; Kang *et al.*, 2019; Lee *et al.*, 2019a; Yang *et al.*, 2019). However, it is an organic composite and may deteriorate when exposed to outdoor environments owing to biological and non-biological factors. Wood undergoes discoloration and decomposition when exposed to light,

i.e., photo-degradation; it also has a shortened service life when exposed to the outdoors for long durations (Borgin, 1971; Evans and Schmalzl, 1989; Kim and Kim, 2020; Kuo and Hu, 1991; Owen *et al.*, 1993; Plackett *et al.*, 1992; Tshabalala and Gangstad, 2003).

One of the major causes of the photo-degradation of wood is that lignin, one of its main components, absorbs UV light, resulting in the migration of radical intermediates and the subsequent formation of quinoid structures (Cogulet *et al.*, 2016; Pandey and Vuorinen, 2008). Also, wood extractives that have double bonds and benzene rings in their structures undergo discoloration (Chang *et al.*, 2010; Fan *et al.*, 2009; Pandey, 2005). Many studies have explored ways to prevent this photo-degradation, among which the most widely used are wood-coatings to block or absorb UV light via UV stabilizers, absorbents, hindered amine light stabilizers (HALS), and quenchers. Most UV absorbents constitute organic matter; however, studies are actively exploring inorganic UV absorbents. Guo *et al.* (2016) and Lozhechnikova *et al.* (2017) coated objects with ZnO nanostructures, an inorganic material that can effectively absorb UV light. Pánek *et al.* (2017) reported wood-coating treatments using ZnO nanoparticles, hydrophobic materials, oils, and UV stabilizers. However, with coating treatments, there are issues such as the discoloration and durability of the coating; in case of UV stabilizers, they only treat the wood surface. Therefore, a simple but effective approach to control or remove the lignin components is essential to mitigate wood discoloration and the subsequent loss in quality.

Various researchers are investigating delignification methods using various solutions containing H_2O_2, $NaClO_2$, NaClO, or Na_2SO_3 to control the lignin content of wood (Khanjanzadeh and Park, 2020; Lee *et al*., 2019b; Park *et al.*, 2018a; Park *et al.*, 2018b; Zendrato *et al*., 2021). Delignification methods that prevent wood photo-degradation can endow the wood with unique properties.

Vasileva *et al.* (2017) at the Royal Swedish Institute of Technology reported a delignification treatment that used NaClO and subsequent polymer impregnation to create transparent wood, demonstrating the potential to create new materials. Kang and Lee (2005) reported improved sound absorption in delignified wood. Various studies have explored partial delignification of wood to alter its thermal conductivity and optical properties and to yield lightweight materials (Chen *et al.*, 2020; Li *et al.*, 2021). Delignification on various wood materials including wood flour are being conducted using chemicals that are used for bleaching in the paper industry to separate wood fibers.

Among the various solutions that are used for bleaching or delignification treatment, peracetic acid (PAA) has strong oxidizing ability and has been reported to promote the oxidation and decomposition of lignin at low temperatures, i.e., below 100℃, with relatively short treatment times (Kang *et al.*, 2015; Ma *et al.*, 2016; Park *et al.*, 2019; Park *et al.*, 2020a; Park *et al.*, 2020b). Following previous studies, this study explored the delignification of wood with a stratified porous structure was conducted using PAA to prevent discoloration of the surface by selectively removing lignin. According to Kataoka (2008), the depth at which discoloration occurs due to degradation caused by weather or UV light does not exceed 34−2,540 μm; therefore, this study aims to use PAA to remove part of the lignin on the wood surface. To compare the extent of delignification among various wood species, the softwood *Larix kaemferi* and the hardwood *Q. mongolica* were employed as the test species. Also, hydrogen peroxide (HP) treatment was additionally conducted for comparison. After the surface chemical treatments, the samples were exposed to artificial UV light to induce photo-degradation, and the changes in the wood color, functional groups and surface images of the samples were observed.

2. MATERIALS and METHODS

2.1. Material

L. kaempferi and *Q. mongolica* (18 years) were used for experimental specimens in this study. Woods were obtained from the academic forest of Kangwon National University in Hongcheon-gun, Gangwon-do, South Korea. *L. kaempferi* is a representative softwood for wooden building, and *Q. mongolica* is the most common hardwood species with the largest dominance in South Korea. Before experiment, wood specimens were prepared with dimensions of 30 (L) × 20 (R) × 40 (T) mm^3 for each chemical treatment. These were conditioned in a climatic chamber at 24℃ and 60% relative humidity. The images of the samples are listed in Fig. 1.

2.2. Methods

2.2.1. Surface chemical treatment

PAA and HP (30%, Daejung, Siheung, Korea) were
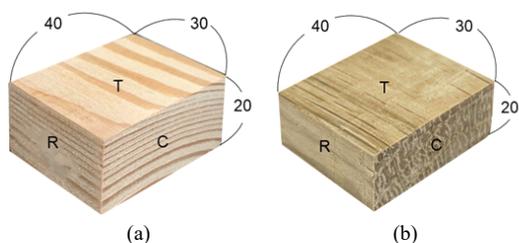
Fig. 1. Wood specimens for experiment. (a) *Larix kaempferi*, (b) *Quercus mongolica*. C: cross section, T: tangential section, R: radial section.

used as solutions for the delignification treatment of the wood surface. In the case of PAA, it was prepared by mixing acetic acid (AA, 99%, Daejung) and HP in a ratio of 1:1.5 (v/v), and the concentration was titrated after storage at room temperature for 2 weeks in order to use the same concentration in the experiment. The concentrations of PAA was measured according to the concentration titration method reported in a previous study (Park *et al.*, 2020a). On the other hand, in order to vary the concentration of the PAA solution, PAA and distilled water were mixed in a ratio of 1:1 (v/v). The concentration of PAA and HP are listed in Table 1. For the chemical treatment, 300 mL of each solution and 3 specimens were placed in a 1 L beaker and reacted at 70℃ for 4, 8 h. After completion of the reaction, it was washed with distilled water and dried in a dark room at room temperature.

2.2.2. Weathering test

After chemical treatment, weathering test was conducted to induce artificial photo-degradation on wood. Weathering conditions were set according to the ASTM G154; A xenon light at 0.89 W/m^2, range of 340 nm, at 60℃, for 168 h in an accelerated weathering tester (QUV/se Accelerated Weathering Tester, Q-LAB, Westlake, OH, USA).

2.2.3. Color measurements

As shown in Fig. 2, the surface color of wood samples for 5 periods was measured using a colorimeter (CR-10 Plus, Konica Minolta, Tyoko, Japan). Color

Table 1. Solution information used for chemical treatment

Condition	Abbreviation	PAA concentration (%)	HP concentration (%)
AA + HP (1:1.5, v/v)	P	9.1	15.7
PAA + D.I water (1:1, v/v)	1/2P	5.8	7.9
HP only	HP	-	30.0

PAA and P: peracetic acid, AA: acetic acid, HP: hydrogen peroxide.

Tangential section
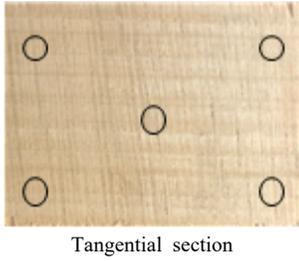
Fig. 2. Measured spots on experimental wood sample (actual sample size).

Table 2. Color difference categorization

Class	Color difference	Color change effect
1	$\Delta E < 0.2$	Invisible changes
2	$0.2 < \Delta E < 2.0$	Very small changes
3	$2.0 < \Delta E < 3.0$	Small changes
4	$3.0 < \Delta E < 6.0$	Medium changes
5	$6.0 < \Delta E < 12.0$	Large changes
6	$12.0 < \Delta E$	Different color

difference measurement were performed both before chemical treatment and after UV irradiation. According to the CIE Lab standard, the L^*, a^*, b^* color coordinates were calculated based on three independent specimens at five different point. ΔL^*, Δa^*, and Δb^* were the total changes of the L^*, a^*, and b^* values during weathering testing, respectively. An increase/decrease in the L^* value means the color of the sample becomes brighter/darker. A positive Δa^* signifies a color shift toward red, and a negative Δa^* signifies a color shift toward green. A positive Δb^* signifies a shift toward yellow, and a negative Δb^* signifies a shift toward blue. The color difference (ΔE) was following Equation (1). And The color difference can be categorized as shown in Table 2 (Hadi *et al.*, 2022).

$$\triangle E^* = \sqrt{(L_0 - L_a)^2 + (a_0 - a_a)^2 + (b_0 - b_a)^2} \tag{1}$$

$L_0 - L_a$, L_0: initial L^* values, L_a: final L^* values.
$a_0 - a_a$, a_0: initial a^* values, a_a: final a^* values.
$b_0 - b_a$, b_0: initial b^* values, b_a: final b^* values.

2.2.4. ATR Fourier transform infrared spectroscopy (FT-IR) analysis

Fourier transform infrared spectroscopy (FT-IR, Nicolet Summit, Thermo Fisher Scientific, Waltham, MA, USA) was used to observe the functional group changes of the specimens after chemical treatment of the wood surface

and UV irradiation. The spectra were recorded in the wavenumber range from 800–2,000 cm^{-1} and 32 scans per sample with a resolution of 4 cm^{-1} were used.

2.2.5. Solution penetration depth

The degree of solution (PAA or HP) penetration depth into the wood after chemical treatment was measured using a vernier caliper. The penetration depth in the longitudinal, radial, and tangential directions was measured 7 times and the average was obtained.

2.2.6. Scanning electron microscope analysis

A scanning electron microscope (SEM, JSM-5510, JEOL, Akishima, Japan) with an accelerating voltage of 3 kV was used to observe changes in the cell wall of the chemically treated specimen. The observation sample was prepared in a size of $5 \times 5 \times 5$ mm^3.

3. RESULTS and DISCUSSION

3.1. Image changes of wood surface

Fig. 3 shows photographs of the wood surfaces to compare the color changes after the PAA and HP treatments at different concentrations and reaction times (4 h and 8 h) as well as the color differences after exposure to UV light.

Visual analysis results revealed that the colors of

Fig. 3. Color changes of *L. kaempferi* (a), *Q. mongolica* (b) after each chemical treatment and artificial UV exposure test. P: peracetic acid, HP: hydrogen peroxide, UV: ultraviolet.

both the tree species tended to lighten compared with control (untreated) when the PAA and HP treatments were performed. Compared to that of HP, more lightening was caused by the PAA treatment, and it was observed that the surfaces of the specimens lightened significantly with increasing solution concentrations and reaction times. Subsequently, the samples were exposed to UV light for 168 h in an accelerated weathering tester; the specimens treated with HP had a dark red color, but the specimens treated with PAA did not show a signi-

ficant color change, demonstrating a wood photo-stabilization effect.

Meanwhile, surface fibers of the specimens treated with PAA showed tearing, indicating that the wood tissue softened considerably due to the delignification (Abdel-Fattah and Abdel-Naby, 2012; Kang *et al.*, 2015; Westin *et al.*, 2021).

In case of the hardwood *Q. mongolica*, the color was close to white after the PAA treatment better than HP treatment, and it experienced less color change after UV

exposure compared to the softwood *L. kaempferi*. The color of *Q. mongolica* treated with PAA was similar at 4 h and 8 h. Therefore, 4 h of PAA treatment resulted in sufficient color stabilization. In the case of the *L. kaempferi*, the specimens treated by PAA turned yellow, and those treated by HP turned dark red. These observations are in accordance with the findings of several other studies that have reported that softwood tree species experience more severe color changes than hardwood tree species (Oberhofnerová *et al.*, 2017; Timar *et al.*, 2016).

3.2. Changes of wood color

3.2.1. Lightness (*L**), redness (*a**), yellowness (*b**), and color difference (⊿*E**)

Surface treatments were performed with varying treatment durations and concentrations of PAA and HP, and changes in wood color caused by the solutions were observed. Thereafter, the samples were exposed to UV light for 168 h, and the wood colors were observed. The lightness (*L**), redness (*a**), yellowness (*b**), and color difference (⊿*E**) values of the *L. kaempferi* and the *Q. mongolica* are shown in Fig. 4 and Fig. 5, respectively.

Both softwood and hardwood specimens exhibited similar tendencies for the same solution concentration and treatment duration except yellowness. In specimens treated with PAA, *L** increased considerably and *a** and *b** decreased. In specimens treated with HP, *L** and *b** increased slightly compared to that in case of PAA and *a** decreased.

After UV exposure, the *L. kaempferi* and the *Q. mongolica* demonstrated decrease in *L** and increase in *a**, but changes in *b** differed for both species. For the *L. kaempferi*, *b** increased after PAA treatment, and it remained the same or decreased after HP treatment. For the *Q. mongolica*, *b** decreased after PAA treatment and increased after HP treatment. Because of this, when the color difference (⊿*E**) was measured, the brown-colored

lignin was found to have a relationship with the *b** value, i.e., yellowness, and it tended to decrease with increasing solution concentration and treatment duration. *b** of the PAA-treated specimens decreased rapidly compared to the untreated wood. *b** decreases because chromophores are destroyed due to structural degradation during delignification (Pan *et al.*, 2000). In contrast, compared to the untreated specimens, *b** increased after HP treatment. This may be because of the structural changes in lignin, i.e., the conversion of benzene rings to quinones, after the HP treatment, which causes an increased reaction to UV light (Chen and Pignatello, 1997; More *et al.*, 2021; Scheck and Frimmel, 1995).

For the PAA-treated specimens, the wood color did not change considerably. Similar to the surface treatment-induced color changes, the UV exposure-induced color changes were smaller in the PAA-treated specimens than in the HP-treated specimens. The color differences (⊿*E**) of PAA-treated wood showed the 4.8−12.2 of *L. kaempferi*, and 1.7−3.7 of *Q. mongolica*, respectively. According to Table 2, under the condition of P-8, *L. kaempferi* is 9.0, which corresponds to large changes, and *Q. mongolica* is 2.4, which corresponds to small changes. Fig. 3(b) shwos that the E value of *Q. mongolica* under the condition P-4 is smaller than the value of P-8. This means that the lignin of *Q. monglica*, hardwood, is easily decomposed and has effective color stabilization even in a short time. Therefore, better wood photo-stabilization was achieved in the *Q. mongolica* sample than in the *L. kaempferi* sample.

This study used PAA, a strong oxidizing agent, for wood color stabilization. A similar study by Park *et al*. (2018a), Park *et al*. (2018b) reported photo-stabilization of wood using NaClO as an alkaline oxidizing agent. Chemical treatments were performed on birch and walnut veneers at 1%, 2%, and 3% concentrations, and the results showed that after exposing the veneers to UV light, the value of ⊿*E** was 5.4 for birch and 4.3 for walnut.
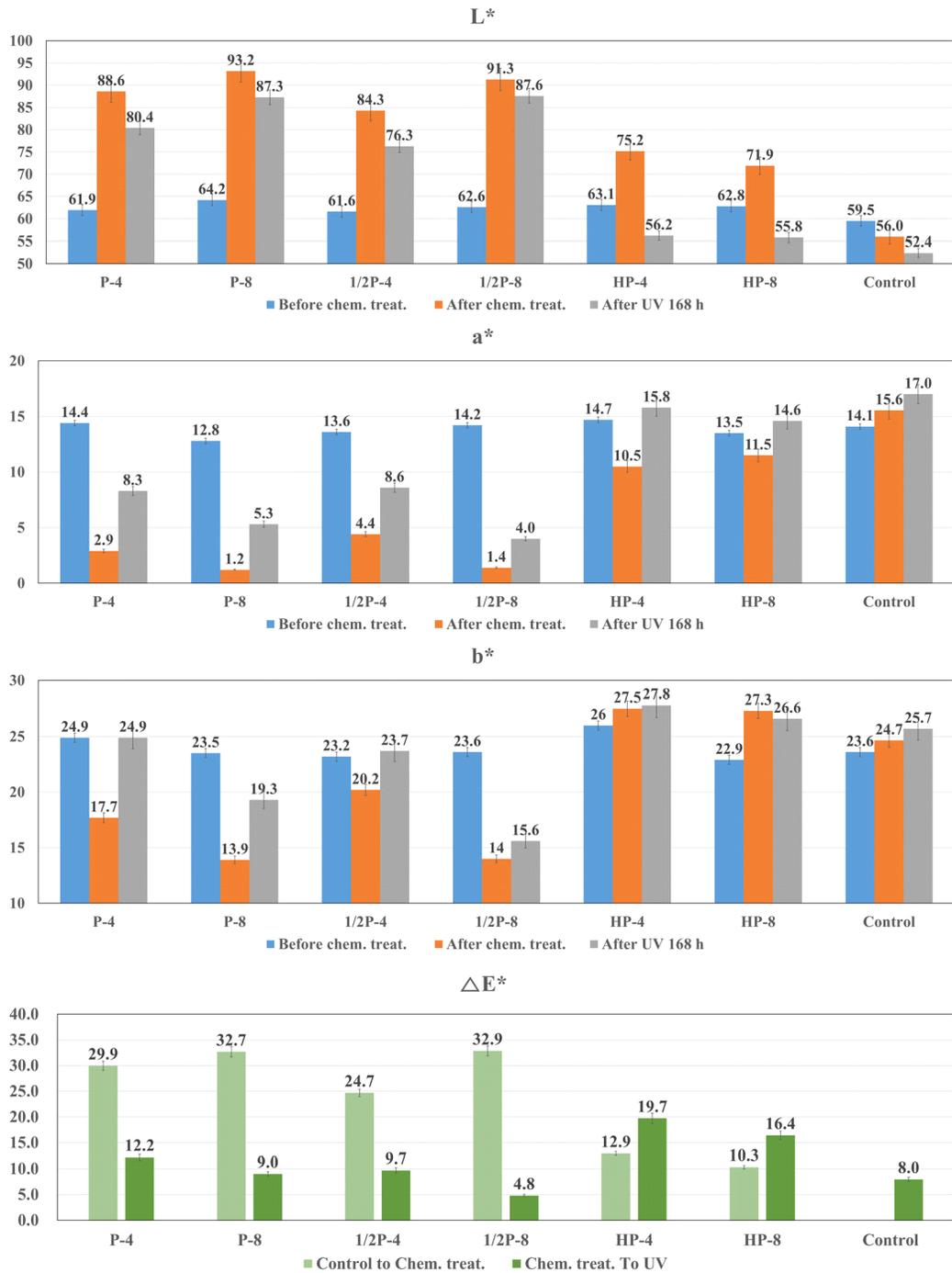
Fig. 4. *L**, *a**, *b**, and △*E** values of *L. kaempferi*.
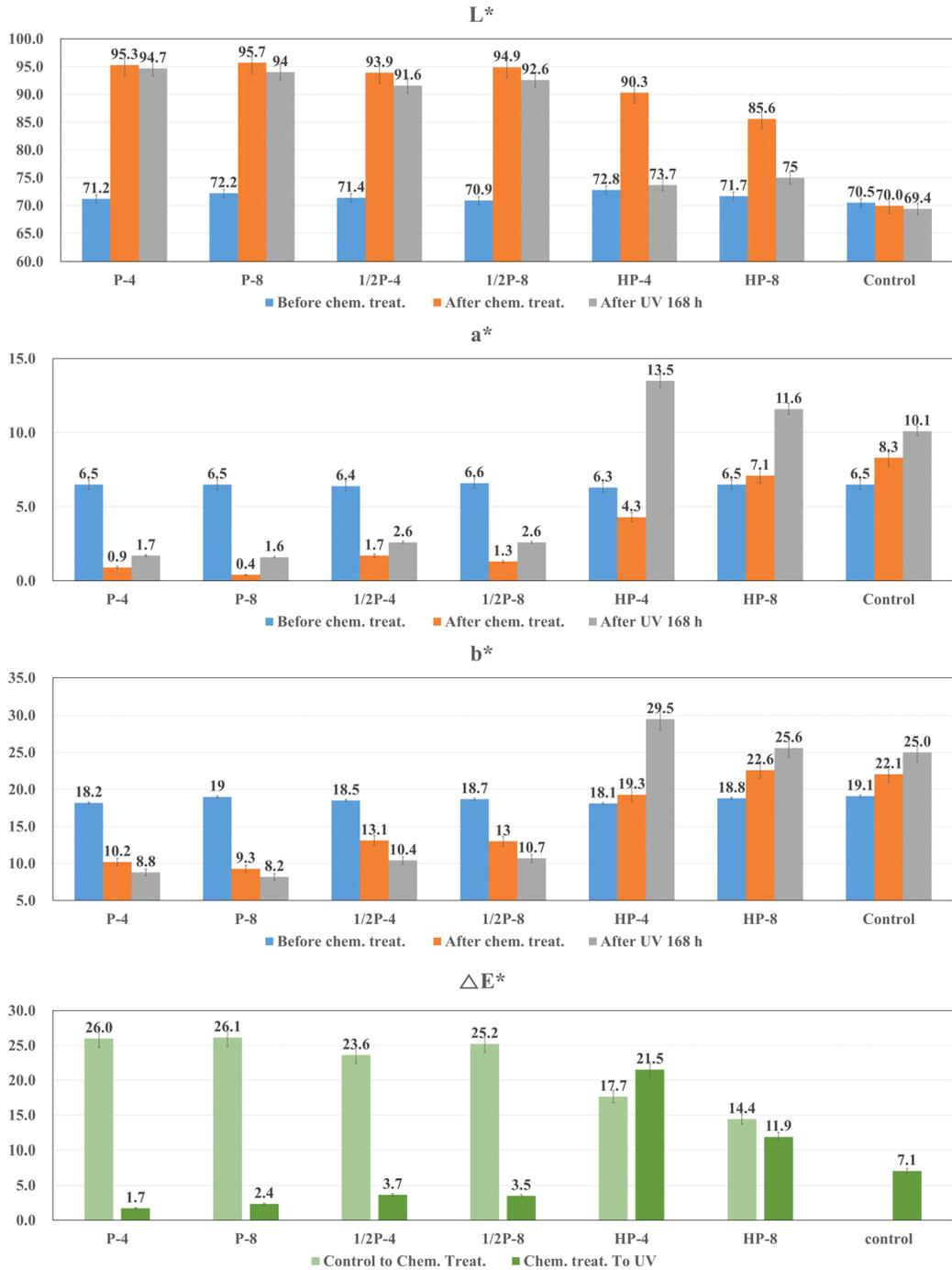
Fig. 5. *L**, *a**, *b**, and $\triangle E^*$ values of *Q. mongolica*.

Another study by Yamamoto et al. (2017) analyzed color differences ($\varDelta E^*$) under acid treatments using distilled water, HP, and alkali mixed in HP. Using a combination of alkali and HP, the $\varDelta E^*$ was 10, and it was 7 using a combination of HP and distilled water. Alkali or alkali mixtures have been typically used in wood color control studies; however, this study used PAA solutions so that the data can be used to compare alkali conditions and acid conditions (Hermansyah *et al.*, 2019).

3.3. Changes of functional group

Fig. 6 shows the functional group changes in the wood surfaces of the untreated sample and the PAA and HP treatment, followed by UV exposure. The analysis was focused in the range of 2,000−800 cm^{-1} to observe changes in the lignin structure caused by the PAA and HP treatments. The functional groups assignments are listed in Table 3. Even though the peak positions are slightly different for the two wood species, the overall shapes of the peaks are similar. The notable difference between the softwood and hardwood is the C = O stretching band at 1,260 cm^{-1}, which was only observed in the guaiacyl lignin of the *L. kaempferi*.

The top of Fig. 7(a) and (b) is a graph of the changes in the peaks of the untreated wood induced by the PAA and the HP treatments. The bottom of Fig. 6(a) and (b) is a graph of the changes caused by exposing the chemically surface-treated specimens to UV light. The
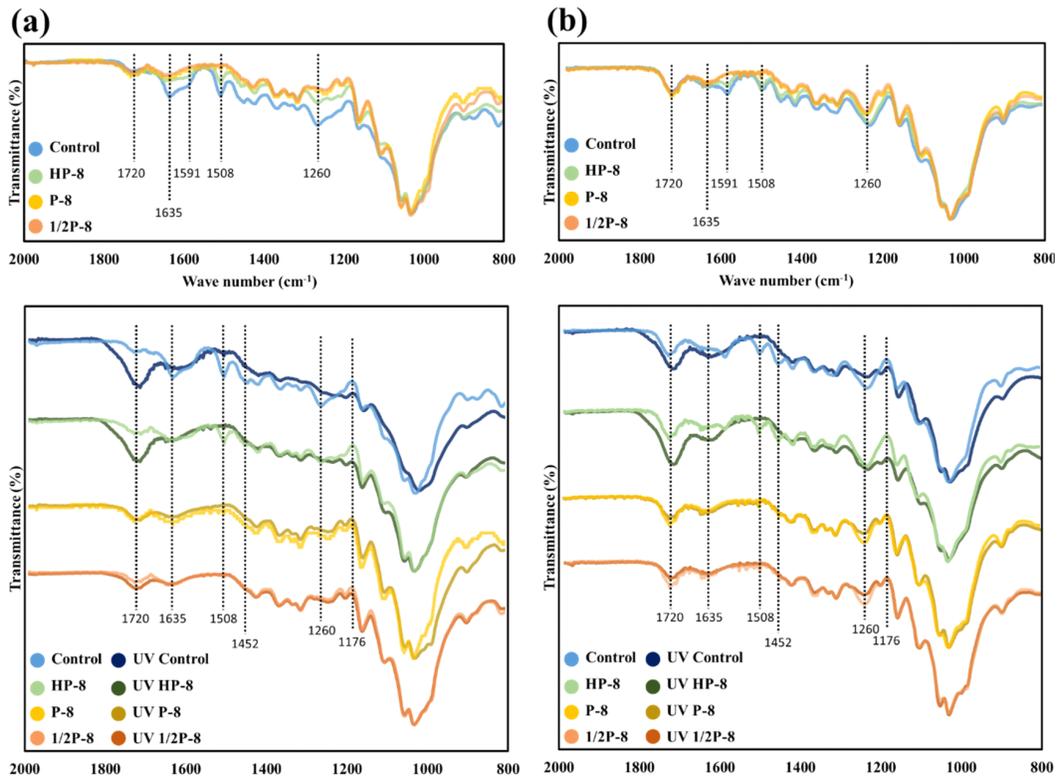
Fig. 6. FTIR transmittance spectra of *L. kaempferi* (a), *Q. mongolica* (b) specimens after chemical treatment and artificial UV exposure. P: peracetic acid, HP: hydrogen peroxide, UV: ultraviolet.

Table 3. Characteristic bands of FT-IR transmittance of *Larix* and *Quercus*

Wavenumber (cm^{-1})		Functionality
L. kaempferi	*Q. mongolica*	
1,720	1,725	Unconjugated C = O in hemicellulose
1,635	1,637	Conjugated C = O in lignin
1,591	1,591	C = O stretching vibration in syringyl lingin
1,508	1,508	C = O stretching vibration in guaiacyl lingin
1,452	1,450	C-H bending vibration in lignin and aromatic carbon skeleton
1,422	1,422	C-H deformation and aromatic ring skeletal vibrations in lignin and carbohydrates
1,365	1,370	C-H deformation in cellulose and hemicellulose
1,314	1,313	C-H vibration in cellulose C-O vibration in syringyl lignin
1,260	1,260	C = O stretching vibration in guaiacyl lingin
1,240	1,241	C-O stretching in hemicellulose and syringyl lignin
1,176	1,180	C-O-C asymmetric bridge stretching in cellulose and hemicellulose
1,104	1,104	C-O-C asymmetric bridge stretching in cellulose and hemicellulose

Reference: Schwanninger *et al.* (2004), Kwon *et al.* (2013), Miranda *et al.* (2012), Zhao *et al.* (2013), Xing and Li (2014), Timar *et al.* (2016), Abdullah *et al.* (2017), Oberhofnerová *et al.* (2017), Vaughn *et al.* (2017), Gonultas and Candan (2018), Yin *et al.* (2018), Zhang *et al.* (2018), Liu *et al.* (2016, 2019), Kubovský *et al.* (2020), Xing *et al.* (2020).
FT-IR: Fourier transform infrared spectroscopy.

cellulose C-O peak at 1,020−1,030 cm^{-1} indicates strong absorption and is not greatly affected, as revealed by FT-IR (Rosu *et al.*, 2010). Therefore, similar to previous studies, intermittent quantitative analysis was performed by fixing the graph at 1,030 cm^{-1} and the changed peaks were observed. During the PAA treatment and artificial UV exposure, considerable changes occurred in the lignin-related functional groups, and small changes were found in the hemicellulose functional groups, indicating that some of the lignin and hemicellulose were partially removed. Specimens treated with PAA by irradiating UV light had no significant change in the aforementioned visual observation and color difference measurement. Also, in the FT-IR analysis, the PAA-treated specimen showed little change by UV light, so it was thought that PAA and UV light reacted with the same functional group. This is the reason for the wood stabilization reaction that occurs as the lignin that responds to UV irradiation is removed.

3.4. Changes of cell wall structure

Fig. 7 shows scanning electron microscopy (SEM) images before and after PAA treatment. The cell walls in untreated samples were shown in the Fig. 7(a) and (c). After PAA treatment, empty spaces were observed between the cells [Fig. 7(b) and (d)]. These are the middle lamella that have high lignin content, and it was visually confirmed that the lignin in the cell walls was removed by the PAA.

Recent delignification studies have focused on the use of partially or completely delignified woods, which
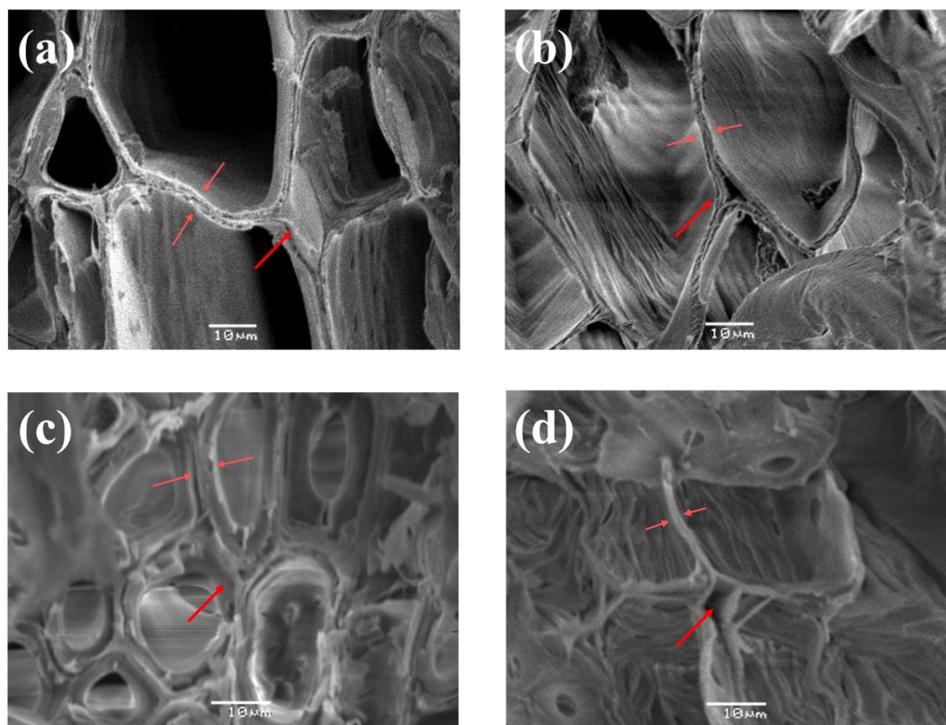
Fig. 7. SEM images. (a) Untreated *L. kaempferi* specimens. (b) P-8-treated *L. kaempferi* specimens. (c) Untreated *Q. mongolica* specimens. (d) P-8-treated *Q. mongolica* specimens. SEM, scanning electron microscope.

has expanded pores within the wood cells. And then, polymer impregnation or functional group modification is easier, resulting in new functional materials. Therefore, the proposed PAA delignification has many potential applications in manipulating cell walls and forming new materials.

3.5. Measurement of delignification depth

Table 4 shows the extent of delignification via the measurement of depths from the surfaces of the two wood species after the chemical treatments. In the case of the PAA-treated specimens, removal of the thickest layer of lignin generally occurred along the direction of the fibers, and the penetration depth was proportional to the increase in concentration of PAA and the reaction

time. This was attributed to the vessels and tracheid cells arranged along the direction of the fibers.

In the HP-treated specimens, which were the comparison group, the delignified areas were not distinct, and so the measurement was not conducted.

When the penetration depths of the two tree species were compared visually (Fig. 8), the delignification depth of *L. kaempferi* was deeper than *Q. mongolica*; however, a clear difference in the earlywood/latewood intermediate part was observed. In contrast, in the case of the *Q. mongolica*, there is a difference in the tissue cells including vessel elements because it is a hardwood species, and relatively uniform delignification was observed in the cross sections. Therefore, PAA treatment conditions should be set according to the wood species.

Table 4. The penetration depth of wood surface after chemical treatment

Species	Conditions	Longitudinal direction (mm)	Tangential direction (mm)	Radial direction (mm)
L. kaempferi	P-4	2.3 (0.96)	1.3 (0.50)	1.8 (0.29)
	P-8	3.3 (0.96)	1.8 (0.50)	4.0 (0.41)
	1/2P-4	1.3 (0.50)	0.9 (0.25)	0.9 (0.25)
	1/2P-8	2.5 (0.58)	1.5 (0.41)	2.0 (0.41)
Q. mongolica	P-4	1.9 (0.63)	1.1 (0.25)	1.6 (0.48)
	P-8	3.0 (0.08)	2.4 (0.48)	3.0 (0.71)
	1/2P-4	0.9 (0.25)	0.5 (0.08)	1.0 (0.08)
	1/2P-8	1.0 (0.08)	1.1 (0.25)	1.6 (0.25)

(a)   (b)
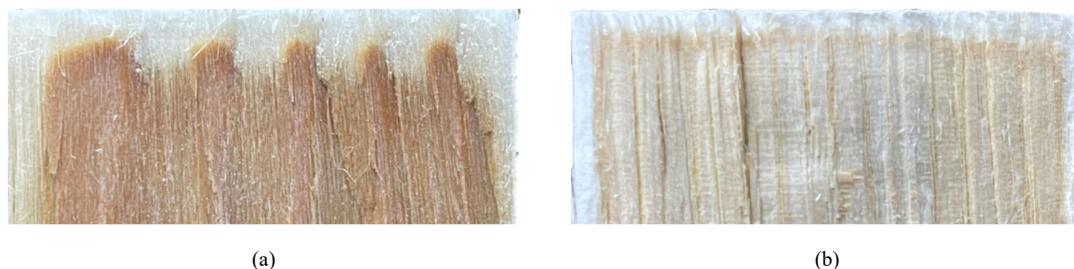
Fig. 8. Internal penetration depth by peracetic acid (8 h condition). (a) *L. kaempferi*, (b) *Q. mongolica*.

4. CONCLUSIONS

PAA and HP were used to perform surface chemical treatments on *L. kaempferi* and *Q. mongolica* specimens, and the treated samples were subsequently exposed to UV light. The following conclusions were obtained from observing the results of the treatments.

1. Visual observations indicated that the colors of both tree species tended to lighten after the surface chemical treatments. After subsequent UV exposure for 168 h, the color difference (ΔE^*) in the PAA-treated *L. kaempferi* was 4.8−12.2, while the color difference in the *Q. mongolica* was 1.7−3.7. These results indicated that PAA treatment gives photo-stabilization effect of wood without significant changes.

2. FT-IR measurements indicated that there were major changes in the lignin-related functional groups as well as minor changes in the hemicellulose functional groups of the specimens treated with PAA. Thus, it can be inferred that some of the lignin and hemicellulose were removed by the surface chemical treatment.

3. SEM images indicated that lignin in middle lamella was removed and the cell walls became thinner, confirming that lignin can be selectively removed by PAA.

4. We determined that PAA can be effectively used for wood photo-stabilization, and it is an important method to control the degree of delignification by adjusting the time and the amount of PAA. Notably, surface tearing occurs during PAA treatment, and various methods such as densification and polymer impregnation can be used to prevent it.

In the future, it is essential to conduct studies on

reducing the cost of the PAA treatment process by exploring ways to improve it and on the finding value-added chemical.

CONFLICT of INTEREST

No potential conflict of interest relevant to this article was reported.

ACKNOWLEDGMENT

REFERENCES

Abdel-Fattah, A.F., Abdel-Naby, M.A. 2012. Pretreatment and enzymic saccharification of water hyacinth cellulose. Carbohydrate Polymers 87(3): 2109-2113.

Abdullah, A.R., Hapidin, H., Abdullah, H. 2017. Phytochemical analysis of *Quercus infectoria* galls extracts using FTIR, LC-MS and MS/MS analysis. Research Journal of Biotechnology 12(12): 55-61.

Borgin, K. 1971. The mechanism of the breakdown of the structure of wood due to environmental factors. Journal of the Institute of Wood Science 5(4): 26-30.

Chang, T.C., Chang, H.T., Wu, C.L., Chang, S.T. 2010. Influences of extractives on the photodegradation of wood. Polymer Degradation and Stability 95(4): 516-521.

Chen, C., Kuang, Y., Zhu, S., Burgert, I., Keplinger, T., Gong, A., Li, T., Berglund, L., Eichhorn, S.J., Hu, L. 2020. Structure‒property‒function relationships of natural and engineered wood. Nature Reviews Materials 5(9): 642-666.

Chen, R., Pignatello, J.J. 1997. Role of quinone intermediates as electron shuttles in Fenton and photoassisted Fenton oxidations of aromatic compounds. Environmental Science & Technology 31(8): 2399-2406.

Cogulet, A., Blanchet, P., Landry, V. 2016. Wood degradation under UV irradiation: A lignin characterization. Journal of Photochemistry and Photobiology B: Biology 158: 184-191.

Evans, P.D., Schmalzl, K.J. 1989. A quantitative weathering study of wood surfaces modified by chromium VI and iron III compounds. Part 1. Loss in zero-span tensile strength and weight of thin wood veneers. Holzforschung 43(5): 289-292.

Fan, Y., Gao, J., Chen, Y. 2009. Colour responses of black locust (*Robinia pseudoacacia* L.) to solvent extraction and heat treatment. Wood Science and Technology 44(4): 667-678.

Fujimoto, Y., Tanaka, H., Morita, H., Kang, S.G. 2021. Development of ply-lam composed of Japanese cypress laminae and Korean larch plywood. Journal of the Korean Wood Science and Technology 49(1): 57-66.

Gonultas, O., Candan, Z. 2018. Chemical characterization and FTIR spectroscopy of thermally compressed eucalyptus wood panels. Maderas. Ciencia y Tecnología 20(3): 431-442.

Guo, H., Fuchs, P., Cabane, E., Michen, B., Hagendorfer, H., Romanyuk, Y.E., Burgert, I. 2016. UV-protection of wood surfaces by controlled morphology fine-tuning of ZnO nanostructures. Holzforschung 70(8): 699-708.

Hadi, Y.S., Herliyana, E.N., Pari, G., Pari, R., Abdillah, I.B. 2022. Furfurylation effects on discoloration and physical-mechanical properties of wood from tropical plantation forests. Journal of the Korean Wood Science and Technology 50(1): 46-58.

Hermansyah, H., Putri, D.N., Prasetyanto, A., Bintang, Z., Chairuddin, M.S.P., Sahlan, M., Yohda, M. 2019. Delignification of oil palm empty fruit bunch using peracetic acid and alkaline peroxide combined with the ultrasound. International Journal of Tech-

nology 10(8): 1523-1532.

Jang, S.S., Lee, H.W. 2019. Lateral resistance of CLT wall panels composed of square timber larch core and plywood cross bands. Journal of the Korean Wood Science and Technology 47(5): 547-556.

Kang, C., Lee, N. 2005. Changes of sound absorption capability and anatomical features of wood by delignification treatment. Journal of the Korean Wood Science and Technology 33(4): 9-14.

Kang, C.W., Jang, S.S., Kang, H.Y., Li, C. 2019. Sound absorption rate and sound transmission loss of CLT wall panels composed of larch square timber core and plywood cross band. Journal of the Korean Wood Science and Technology 47(1): 33-39.

Kang, J.W., Doo, Y.S., Jeong, M.J., Kang, K.Y. 2015. The quantitative analysis of solutes from the peracetic acid pretreatment of wood chips. In: Daegu, Korea, Proceedings of Korea Technical Association of the Pulp and Paper Industry, pp. 102-103.

Kataoka, Y. 2008. Photodegradation of wood and depth profile analysis. Mokuzai Gakkai-Shi 54(4): 165-173.

Khanjanzadeh, H., Park, B.D. 2020. Characterization of carboxylated cellulose nanocrystals from recycled fiberboard fibers using ammonium persulfate oxidation. Journal of the Korean Wood Science and Technology 48(2): 231-244.

Kim, G.C., Kim, J.H. 2020. Changes in mechanical properties of wood due to 1 year outdoor exposure. Journal of the Korean Wood Science and Technology 48(1): 12-21.

Kubovský, I., Kačíková, D., Kačík, F. 2020. Structural changes of oak wood main components caused by thermal modification. Polymers 12(2): 485.

Kuo, M., Hu, N. 1991. Ultrastructural changes of photodegradation of wood surfaces exposed to UV. Holzforschung 45(5): 347-353.

Kwon, S.M., Jang, J.H., Lee, S.H., Park, S.B., Kim, N.H. 2013. Change of heating value, pH and FT-IR spectra of charcoal at different carbonization tempe-

ratures. Journal of the Korean Wood Science and Technology 41(5): 440-446.

Lee, H.W., Jeong, H., Ju, Y.M., Youe, W.J., Lee, J., Lee, S.M. 2019a. Pyrolysis properties of lignins extracted from different biorefinery processes. Journal of the Korean Wood Science and Technology 47(4): 486-497.

Lee, I.H., Song, Y.J., Song, D.B., Hong, S.I. 2019b. Results of delamination tests of FRP- and steel-plate-reinforced larix composite timber. Journal of the Korean Wood Science and Technology 47(5): 655-662.

Li, J., Chen, C., Zhu, J.Y., Ragauskas, A.J., & Hu, L. (2021). *In situ* wood delignification toward sustainable applications. Accounts of Materials Research 2(8): 606-620.

Liu, R., Zhu, H., Li, K., Yang, Z. 2019. Comparison on the aging of woods exposed to natural sunlight and artificial xenon light. Polymers 11(4): 709.

Liu, X.Y., Timar, M.C., Varodi, A.M., Sawyer, G. 2016. An investigation of accelerated temperature-induced ageing of four wood species: Colour and FTIR. Wood Science and Technology 51(2): 357-378.

Lozhechnikova, A., Bellanger, H., Michen, B., Burgert, I., Österberg, M. 2017. Surfactant-free carnauba wax dispersion and its use for layer-by-layer assembled protective surface coatings on wood. Applied Surface Science 396: 1273-1281.

Ma, R., Guo, M., Lin, K., Hebert, V.R., Zhang, J., Wolcott, M.P., Zhang, X., Quintero, M., Ramasamy, K.K., Chen, X., Zhang, X. 2016. Peracetic acid depolymerization of biorefinery lignin for production of selective monomeric phenolic compounds. Chemistry: A European Journal 22(31): 10884-10891.

Miranda, I., Gominho, J., Pereira, H. 2012. Cellular structure and chemical composition of cork from the Chinese cork oak (*Quercus variabilis*). Journal of Wood Science 59(1): 1-9.

More, A., Elder, T., Jiang, Z. 2021. A review of lignin

hydrogen peroxide oxidation chemistry with emphasis on aromatic aldehydes and acids. Holzforschung 75(9): 806-823.

Oberhofnerová, E., Pánek, M., García-Cimarras, A. 2017. The effect of natural weathering on untreated wood surface. Maderas. Ciencia y Tecnología 19(2): 173-184.

Owen, J.A., Owen, N.L., Feist, W.C. 1993. Scanning electron microscope and infrared studies of weathering in southern pine. Journal of Molecular Structure 300(1993): 105-114.

Pan, G.X., Spencer, L., Leary, G.J. 2000. A comparative study on reactions of hydrogen peroxide and peracetic acid with lignin chromophores. Part 2. The reaction of stilbene-type model compounds. Holzforschung 54(2): 153-158.

Pandey, K.K. 2005. A note on the influence of extractives on the photo-discoloration and photo-degradation of wood. Polymer Degradation and Stability 87(2): 375-379.

Pandey, K.K., Vuorinen, T. 2008. Comparative study of photodegradation of wood by a UV laser and a xenon light source. Polymer Degradation and Stability 93(12): 2138-2146.

Pánek, M., Oberhofnerová, E., Zeidler, A., Šedivka, P. 2017. Efficacy of hydrophobic coatings in protecting oak wood surfaces during accelerated weathering. Coatings 7(10): 172.

Park, S.Y., Cho, S.M., Kim, J.C., Hong, C., Kim, S.H., Ryu, G.H., Choi, I.G. 2019. Effects of peracetic acid and hydrogen peroxide concentration on kraft lignin degradation at room temperature. BioResources 14(2): 4413-4429.

Park, S.Y., Choi, J.H., Cho, S.M., Choi, J.W., Choi, I.G. 2020b. Structural analysis of open-column fractionation of peracetic acid-treated kraft lignin. Journal of the Korean Wood Science and Technology 48(6): 769-779.

Park, S.Y., Choi, J.H., Kim, J.H., Cho, S.M., Yeon, S.,

Jeong, H., Lee, S.M., Choi, I.G. 2020a. Peracetic acid-induced kraft lignin solubilization and its characterization for selective production of macro-molecular biopolymers. International Journal of Biological Macromolecules 161: 1240-1246.

Park, S.Y., Hong, C.Y., Kim, S.H., Choi, J.H., Kwon, O., Lee, H.J., Choi, I.G. 2018a. Photodegradation of natural wood veneer and studies on its color stabilization for automotive interior materials. Journal of Wood Chemistry and Technology 38(4): 301-312.

Park, S.Y., Hong, C.Y., Kim, S.H., Choi, J.H., Lee, H.J., Choi, I.G. 2018b. Studies on photoprotection of walnut veneer exposed to UV light. Journal of the Korean Wood Science and Technology 46(3): 221-230.

Plackett, D.V., Dunningham, E.A., Singh, A.P. 1992. Weathering of chemically modified wood. Holz als Roh-und Werkstoff 50: 135-140.

Rosu, D., Teaca, C.A., Bodirlau, R., & Rosu, L. (2010). FTIR and color change of the modified wood as a result of artificial light irradiation. Journal of Photochemistry and Photobiology B: Biology, 99(3): 144-149.

Scheck, C.K., Frimmel, F.H. 1995. Degradation of phenol and salicylic acid by ultraviolet radiation/hydrogen peroxide/oxygen. Water Research 29(10): 2346-2352.

Schwanninger, M., Rodrigues, J.C., Pereira, H., Hinterstoisser, B. 2004. Effects of short-time vibratory ball milling on the shape of FT-IR spectra of wood and cellulose. Vibrational Spectroscopy 36(1): 23-40.

Timar, M.C., Varodi, A.M., Gurău, L. 2016. Comparative study of photodegradation of six wood species after short-time UV exposure. Wood Science and Technology 50(1): 135-163.

Tshabalala, M.A., Gangstad, J.E. 2003. Accelerated weathering of wood surfaces coated with multifunctional alkoxysilanes by sol-gel deposition. Journal of Coatings Technology 75(943): 37-43.

Vasileva, E., Li, Y., Sychugov, I., Mensi, M., Berglund, L., Popov, S. 2017. Lasing from organic dye molecules embedded in transparent wood. Advanced Optical Materials 5(10): 1700057.

Vaughn, S.F., Kenar, J.A., Tisserat, B., Jackson, M.A., Joshee, N., Vaidya, B.N., Peterson, S.C. 2017. Chemical and physical properties of *Paulownia elongata biochar* modified with oxidants for horticultural applications. Industrial Crops and Products 97: 260-267.

Westin, P.O., Yang, X., Svedberg, A., Grundberg, H., Berglund, L.A. 2021. Single step PAA delignification of wood chips for high-performance holocellulose fibers. Cellulose 28(3): 1873-1880.

Xing, D., Li, J. 2014. Effects of heat treatment on thermal decomposition and combustion performance of *Larix* spp. wood. BioResources 9(3): 4274-4287.

Xing, D., Li, J., Wang, S. 2020. Comparison of the chemical and micromechanical properties of *Larix* spp. after eco-friendly heat treatments measured by *in situ* nanoindentation. Scientific Reports 10(1): 4358.

Yamamoto, A., Rohumaa, A., Hughes, M., Vuorinen, T., Rautkari, L. 2017. Surface modification of birch veneer by peroxide bleaching. Wood Science and Technology 51(1): 85-95.

Yang, I., Jeong, H., Lee, J.J., Lee, S.M. 2019. Relationship between lignin content and the durability of wood pellets fabricated using *Larix kaempferi C.* Sawdust. Journal of the Korean Wood Science and Technology 47(1): 110-123.

Yin, X., Huang, A., Zhang, S., Liu, R., Ma, F. 2018. Identification of three *Dalbergia* species based on differences in extractive components. Molecules 23(9): 2163.

Zendrato, H.M., Devi, Y.S., Masruchin, N., Wistara, N.J. 2021. Soda pulping of torch ginger stem: Promising source of nonwood-based cellulose. Journal of the Korean Wood Science and Technology 49(4): 287-298.

Zhang, Y., Yang, L., Wang, D., Li, D. 2018. Structure elucidation and properties of different lignins isolated from acorn shell of *Quercus variabilis* Bl. International Journal of Biological Macromolecules 107: 1193-1202.

Zhao, Q., Nakashima, J., Chen, F., Yin, Y., Fu, C., Yun, J., Shao, H., Wang, X., Wang, Z.Y., Dixon, R.A. 2013. *Laccase* is necessary and nonredundant with peroxidase for lignin polymerization during vascular development in Arabidopsis. The Plant Cell 25(10): 3976-3987.